

Advanced potential field analysis applied to Mise-à-la-Masse surveys for leakage detection

Benjamin Mary^{1,2}, Luca Peruzzo², Yuxin Wu² and Giorgio Cassiani¹

¹Dipartimento di Geoscienze, Università degli Studi di Padova, Via G. Gradenigo 6, 35131 Padova, Italy.

²Earth and Environmental Sciences Area, Lawrence Berkeley National Laboratory, United States

Key Points:

- We have developed the potential field imaging theory to estimate the depth of current sources in Mise-à-la-masse surveys
- Synthetic and field applications of a landfill leakage is demonstrated
- An Open-source code for inversion of voltage using potential field imaging theory is provided.

Corresponding author: Benjamin Mary, benjamin.mary@unipd.it

This article has been accepted for publication and undergone full peer review but has not been through the copyediting, typesetting, pagination and proofreading process, which may lead to differences between this version and the [Version of Record](#). Please cite this article as [doi: 10.1029/2022JB024747](https://doi.org/10.1029/2022JB024747).

This article is protected by copyright. All rights reserved.

Accepted Article

Abstract

Traditionally interpretation of MALM is limited to the visualisation of equipotential contours in order to infer qualitatively the extent of the anomaly. Mise-à-la-masse (MALM) inversion algorithms rely on having a good knowledge of the electrical resistivity distribution in the subsoil. Conversely, potential imaging methods have shown their strength for several applications to quickly estimate the depth of sources even in highly heterogeneous media. In the case of the MALM method, the physics may be described by Poisson's equation. As the conductivity term is modulating the flux of current, MALM is generally referred to as a pseudo-potential method. In this work, we have tested, for the first time, the application of the potential field theory to MALM in order to identify the current source depth. Synthetic modelling shows that the proposed algorithm is effective and efficient, using surface voltage measurements for different resistivity contrasts, anomaly depths and noise levels. We then applied the method to the real field case of a landfill leakage and showed how very different source depth estimates result from an intact or a damaged landfill liner.

Plain Language Summary

The so-called Mise-à-la-Masse (MALM) technique is a well-known active geo-electrical prospecting method aimed at imaging (qualitatively) electrically conductive (often ore) bodies in the subsurface. The current is injected in the core of the body to prospect, and the high electrical conductivity of the body channels the current making it detectable from the anomalies of electrical potential measured, e.g., at the ground surface. Verification of landfill liner integrity is one of the most recent applications of MALM, exploiting the electrical and hydraulic separation, often made with a plastic liner, between the conductive waste inside and the soil outside. Holes in the liner may be imaged inducing a passage of DC current between the inner and the outer part of the landfill, provided that the location of such holes be identified using an efficient MALM inversion. For this purpose, we adapted an algorithm used for voltage inversion to MALM: the approach has proven effective using synthetic modelling and was successfully applied to real field data from an industrial landfill.

1 Introduction

The Mise-à-la-Masse (MALM) method is a variation of the classical geo-electrical investigation approaches, in which DC current is injected into the ground by two electrodes and the difference is measured between two other points. MALM was originally developed to delineate the shape of electrically conductive mineral bodies for mining exploration purposes (Parasnis, 1967; Schlumberger, 1920). MALM traditional implementation assumes that the conductive (ore) body channels current in such an effective manner so that the characteristics of the surrounding medium are irrelevant and interpretation can be limited to the qualitative shape of the voltage map distribution, the contour isolines giving an estimate of the anomaly extent and orientation. This classic MALM approach has found different applications in recent times, in situations where it is useful to verify the electrical connection between one portion and another of the subsoil (e.g. De Carlo et al., 2013; Mary et al., 2020, 2018; Perri et al., 2018; Peruzzo et al., 2020). The MALM approach holds under the assumptions that the contrast between the conductive body and the background is high and that the conductive body is accessible and has a relatively large volume. Applications at landfill bodies are of particular interest where the aim is to verify the connection between the inside and outside of the waste mass, e.g. in presence of a plastic liner which represents, when undamaged, both a hydraulic and an electrical barrier. In this type of application, the interpretation of MALM data is often non-trivial and requires modelling of DC current flow and a reconstruction of the, often poorly known, subsoil heterogeneities. A

62 number of different approaches have been proposed and used to this end, in particular
63 in search for the depth of localized anomaly sources (Binley et al., 1999; Wondimu et
64 al., 2018; Shao et al., 2018; Ling et al., 2019; Mary et al., 2020; Peruzzo et al., 2020).
65 A priori information is always needed to guide the result (de Villiers et al., 2019) and
66 a correction for the influence of the resistivity on the current density distribution is
67 needed.

68 A large body of literature exists regarding potential field imaging using non-
69 iterative (i.e. no inversion in a strict sense) processing, to estimate the location and
70 depth of sources. Up to now, potential field imaging tools have been reserved to
71 passive methods analysis such as self-potential, gravity or magnetic surveys. Patella
72 (1997) formulated an approach to self-potential (SP) data interpretation where the
73 inverse problem is solved using cross-correlation of the field with a scanning source
74 (the electric field generated by an elementary positive charge). Lapenna et al. (2000)
75 applied that approach to outline the SP source geometry and dynamics within a faulted
76 structure. In their review article, Fedi and Pilkington (2012) discuss a number of
77 existing algorithms and note that all such methods have in common two steps: the
78 upward continuation of the field and a depth weighting factor (scaling function) to
79 identify the source location.

80 The upward continuation of the field is generally performed via Fourier transfor-
81 mation. An alternative powerful approach is the use of Continuous Wavelet Transform
82 (CWT - Bhattacharya & Roy, 1981; Gibert & Pessel, 2001; Abdelrahman, El-Araby,
83 Abo-Ezz, Soliman, & Essa, 2008; Agarwal & Srivastava, 2009; Srivastava & Agarwal,
84 2010; Saracco, Labazuy, & Moreau, 2004).

85 Among other algorithms, the so-called Depth from Extreme Points (DEXP -
86 Fedi, 2007; Fedi, Florio, & Cascone, 2007) has been especially conceived with the
87 possibility of using the field spatial derivatives to improve the resolution and a more
88 accurate weighting law depending on the so-called Structural Index (SI) of the source.
89 An automatic DEXP imaging method independent from the value of the SI of the
90 causative source was also proposed later to add flexibility to the procedure (Abbas &
91 Fedi, 2014; Abbas et al., 2014). More recently, Baniamerian et al. (2016) introduced
92 the compact-DEXP (CDEXP) algorithm for fast modelling the potential field anomaly.
93 The DEXP transformation and the Continuous Wavelet Transform belong to different
94 theories but present some similarities (Fedi et al., 2010; Fedi & Pilkington, 2012). The
95 key difference between DEXP and CWT is the respective choices of the power-law
96 exponent. In the DEXP case, the exponent depends on the differentiation order and
97 the source properties (through the SI), while in the CWT formulation the exponent
98 depends only on the differentiation order (Revil, 2013). Fedi (2007) discussed the
99 pro and cons of using an imaging against an inversion approach for source depth
100 estimation, since inversion codes of natural potential field also proved their efficiency
101 for spontaneous potential (Soueid Ahmed et al., 2013) and gravity (Fedi, 2007; Florio &
102 Fedi, 2018). Note that Fedi et al. (2010) show that for CWT (and DEXP) the influence
103 of a heterogeneous resistivity distribution (three orders of magnitude differences) is
104 negligible on source depth estimation. As suggested by Liu et al. (2020), the imaged
105 model (using CWT or DEXP) may always be used as a reference or a starting model
106 during a subsequent inversion process.

107 In this paper we describe a new approach that uses the DEXP theory to interpret
108 MALM surveys to derive approximate source location. The main steps involve (a)
109 synthetic modelling in order to verify to what extent the physics governing MALM
110 is compatible with the potential theory imaging method (reported in the Supporting
111 Information); (b) application of the modified DEXP algorithm (in the sequel, named
112 pyDEXP) to a synthetic and a real MALM datasets, both related to the identification
113 of leakage from an industrial landfill.

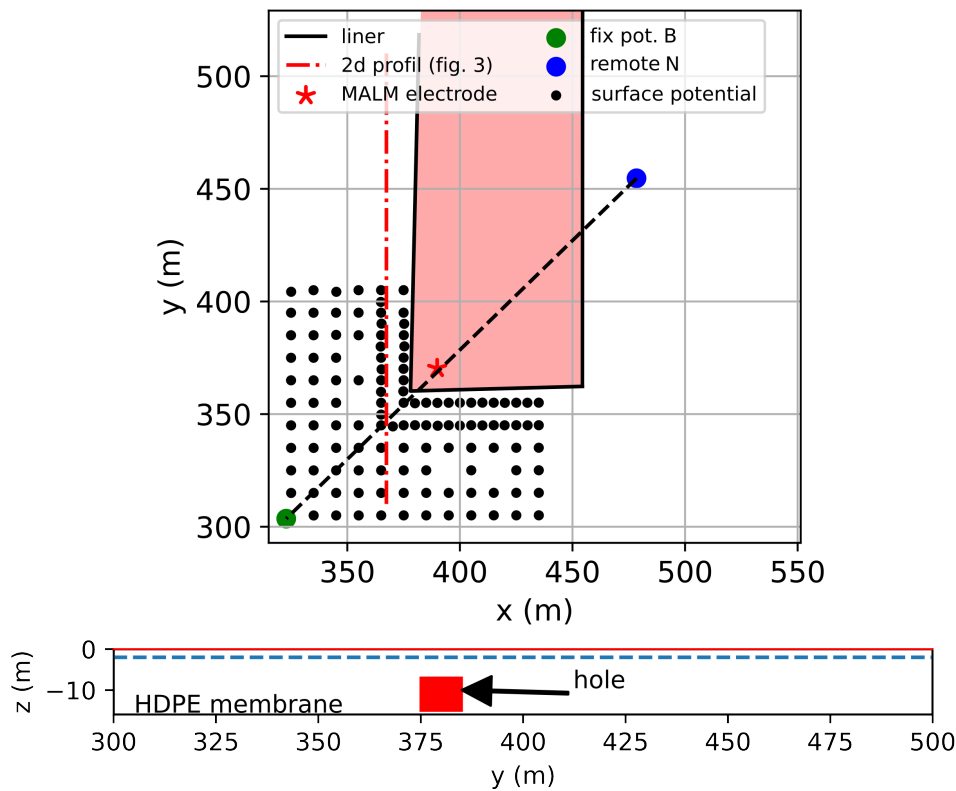


Figure 1. Geometry of the landfill case study: only the South-East corner, around which a leak in the vertical liner was suspected, is sketched here. The inner part of the landfill corresponds to the blurred red area of the figure. Dashed red line show the symmetry of the survey with A, B and M electrodes aligned. Depth section (yz) showing the possible location and size of the hole (red square) and the position of the water table (dashed blue line)

2 Case study

The case study we present concerns an industrial landfill in Northern Italy, having the following characteristics:

1. The contaminated part of the site consists of an area of about 2 hectares surrounded by a physical barrier, 16 m deep, made of a trench filled with clayey material having an embedded vertical HDPE (plastic) membrane. The water table is positioned practically at the ground surface. No bottom liner exists.
2. The sediments are silty, saturated by brackish water for which we can assume an electrical conductivity of about $0.5 S/m$. Assuming a reasonable formation factor of 5, we expect the saturated formation to have an electrical conductivity of about $0.1 S/m$, i.e. an electrical resistivity of $10 \Omega.m$.
3. Given the presence of brackish water, one can assume that the resistivity of the entire system, inside and outside the landfill body, is homogeneous and equal to $10 \Omega.m$, with the single most notable exception of the barrier itself, where the HDPE lines corresponds to an exceedingly large resistivity anomaly (fig 1).

129 The current injection electrode A was placed 12 m deep in a monitoring borehole
 130 inside the landfill (fig 1). The current return electrode B and the reference voltage
 131 electrode N were placed remotely while the rover voltage electrode M was moved on a
 132 regular grid of 10x10 m (fig 1). The fixed electrodes A, B, N all lie on the diagonal of
 133 the South-East corner of the landfill (fig 1): in this way any lack of symmetry of the
 134 resulting voltage measured at the ground surface would be indicative of a discontinuity
 135 in the HDPE barrier. Note that current can flow anyway from the interior to the
 136 exterior of the landfill primarily below the lateral barrier, at a depth of about 16 m
 137 from the ground surface, where the HDPE liner ends. Therefore, in absence of any
 138 liner discontinuity, the voltage map at the surface should be symmetric with respect to
 139 the diagonal of the landfill corner. MALM data were collected in October 2019 using a
 140 Syscal Pro (Iris instrument). Both normal and reciprocal configurations (e.g. Binley,
 141 Ramirez, & Daily, 1995) were collected in order to ensure optimal data quality. The
 142 details of the synthetic modelling for survey design, of data processing and imaging
 143 using DEXP are given in the Supporting Information.

144 3 Methods

145 3.1 Upward continuation of the potential field

146 The first step common to all potential field processing methods consists in creat-
 147 ing a 3D potential field from the data measured along a surface (typically, the ground
 148 surface at $z=0$) and is performed in this study via upward continuation of the sur-
 149 face data u . This is possible because no source of potential field is present above the
 150 ground surface. Blakely (1995) formulates the continuation through the Fast Fourier
 151 Transform in the wavenumber domain as:

$$152 F(U_{up}) = F(u)e^{-\Delta z|k|}, \quad (1)$$

153 and then transformed back to the space domain. U_{up} is the upward continued data,
 154 Δz is the height above the measurement plane, F denotes the Fourier Transform, and
 155 $|k|$ is the wavenumber modulus. A particular attention must be given to assigning the
 right input parameters with regards to the resolution needed, i.e. the z discretization.

156 3.2 Analysis of the field and its derivatives by the DEXP method

157 Among all possible ways to analyse the potential field, we propose here an im-
 158 plementation of the DEXP method, as this is flexible enough to estimate source depth
 159 density from MALM data and provide a fast image of the source possible distribution.
 160 In particular, we take advantage of its automatic Structural Index identification and
 161 its good resolution using the derivatives of the potential field.

162 The final step consists in scaling the field in order to obtain the depth of the
 163 source via the DEXP transformation. Fedi (2007) defined the DEXP transformation
 164 as:

$$165 \Omega(r, z_i) = \left| z_i^{\frac{N}{2}} \right| U_{up}(r, z_i) \quad (2)$$

166 with $i=1, \dots, L$, and where $\Omega(r, z_i)$ is the DEXP-scaled field at the elevation z_i , $U_{up}(r, z_i)$
 167 is the field u upward continued at z_i (with i being the layer number ranging from 1
 168 to L) and $z_i^{\frac{N}{2}}$ is the DEXP power law. Applying the DEXP transformation to the
 169 q^{th} order vertical derivative of the field, results in new DEXP operators (Fedi et al.,
 2010):

$$\Omega^{(q)}(r, z_i) = \left| z_i^{\frac{(q+N)}{2}} \frac{\partial^q U_{up}(r, z_i)}{\partial z^q} \right|_{z=z_i} \quad (3)$$

and

$$\Omega^{(q)}(r, z_i) = \left| z_i^{\frac{(q+N)}{2}} \frac{\partial^q U_{up}(r, z_i)}{\partial x \partial z^{q-1}} \right|_{z=z_i} \quad (4)$$

with $i=1, \dots, L$.

Horizontal derivatives can be computed via finite difference or Fast Fourier Transform (FFT) calculation. On the contrary, for stability reasons only FFT can be used for the vertical derivative computation. A set of “ridges” that, according to Fedi’s theory (2007), are the extrema of the field and the vertical and horizontal derivatives of the upward continued field are formed. In this study, we refer to ridge types I and II respectively where the field horizontal or vertical derivative is zero, and ridge type III where the field itself is zero. While it was possible to consider analysis of ridges in order to define the structural index (N), we rather implemented the automatic DEXP method (Abbas & Fedi, 2014). The key point in eq. 5 below is that the DEXP ratio R_{mn} is independent of the structural index (N) and depends only on known quantities m and n , that is the difference between the orders of the field derivatives f_m and f_n .

$$R_{mn} = \frac{f_m}{f_n} \quad (5)$$

$$\Omega(R_{mn}) = z^{\frac{(m-n)}{2}} R_{mn} \quad (6)$$

3.3 MALM and the potential field theory

In order to process the MALM data, first of all we need to define the physics of the problem. At steady state, the governing partial differential equation (PDE) for the direct current problem is:

$$\nabla \cdot \sigma \nabla V = -I \delta(r) \quad (7)$$

where $\delta(r)$ indicates the Dirac delta positioned at coordinates r and thus indicating point current injection source(s). The voltage in resistivity methods is actually a pseudo-potential since it is modulated by the conductivity σ . If the conductivity of the medium is homogeneous the partial differential equation (PDE) simplifies to Poisson’s equation:

$$\Delta V = I \delta(r) \quad (8)$$

And in absence of current sources to Laplace’s equation:

$$\Delta V = 0 \quad (9)$$

The analogy of these equations with those of the gravitational field is, of course, apparent (i.e. given the gravitational potential U , the relevant governing equation is $\Delta U = -4\pi\gamma\rho$ where ρ is density and γ is the gravitational constant). In order to correct for the influence of the return current electrode, thus removing the relevant

197 voltage contribution, we computed this contribution via the simple calculation of the
198 potential V at a point P for a homogeneous soil in a semi-infinite conductor:

$$V(P) = \frac{I}{2\pi l} \quad (10)$$

199 with I being the intensity of the current injected, and l the distance between the
200 injection point and the point P .

201 4 MALM imaging results on the landfill

202 4.1 Voltage distribution

203 The resulting voltage distribution in the actual MALM experiment is shown in
204 figure 2 and compared against the results of the synthetic analogue used for survey
205 design (see Supporting Information).

206 The simulated voltage for the synthetic case clearly shows how the presence of a
207 discontinuity in the HDPE vertical liner is visible in terms of voltage distribution on
208 the ground surface (compare fig 2a and fig 2b). In the simulations the hole is 10 m
209 wide and 8 m high, and its top is at 12.5 m depth from the ground surface.

210 Figure 2c shows the synthetic results for the damaged liner case after mirroring
211 (see Supporting Information for details) along the line parallel to the Southern border
212 of the landfill (see fig 1). The procedure is needed in order to confirm the data (available
213 in practice only outside of the landfill) with the theory that is designed to look for a
214 point-like anomaly along a vertical plane of symmetry.

215 As for the field data, a comparison between figures 2d and 2e shows how the
216 correction for the influence of the current return electrode location changes the pattern
217 and the amplitude of the normalised voltage distribution. After correction, the field
218 data show with more evidence that the anomaly of electrical potential propagates
219 outside the landfill area. Similar to the synthetic data, mirroring of the field data
220 around the landfill lateral wall is needed for multi-ridge analysis as described in the
221 DEXP approach (fig 2f).

222 4.2 Estimation of leak point from field data

223 The multi-ridge analysis in the DEXP approach is designed to identify the loca-
224 tion of the source at depth. We conducted such an analysis using the MALM voltages
225 collected during the field survey in a totally analogous manner as for the synthetic
226 data described in the Supporting Information. The analysis is conducted in 2D along
227 the line of Southern side of the landfill (fig 1). However, for the field data, many ridges
228 appeared to be inconsistent disturbing their intersections. We cannot reach conclu-
229 sions concerning the source depth based only on the geometrical analysis of the ridge
230 intersections. However, the ratio DEXP analysis shows the source at approximately
231 8m depth (fig 3).

232 5 Discussion

233 The use of the potential field imaging theory for the identification of MALM
234 source depth due to current leakage (in the specific case, from a landfill) has pros and
235 cons. When applied to passive prospection methods (such as self-potential or gravime-
236 try), potential methods seek for a naturally induced source at depth. Conversely, in
237 the MALM case, the field is induced by current injection via a pair of electrodes. The
238 current propagates through the conductive body and is then diffused to the soil. In

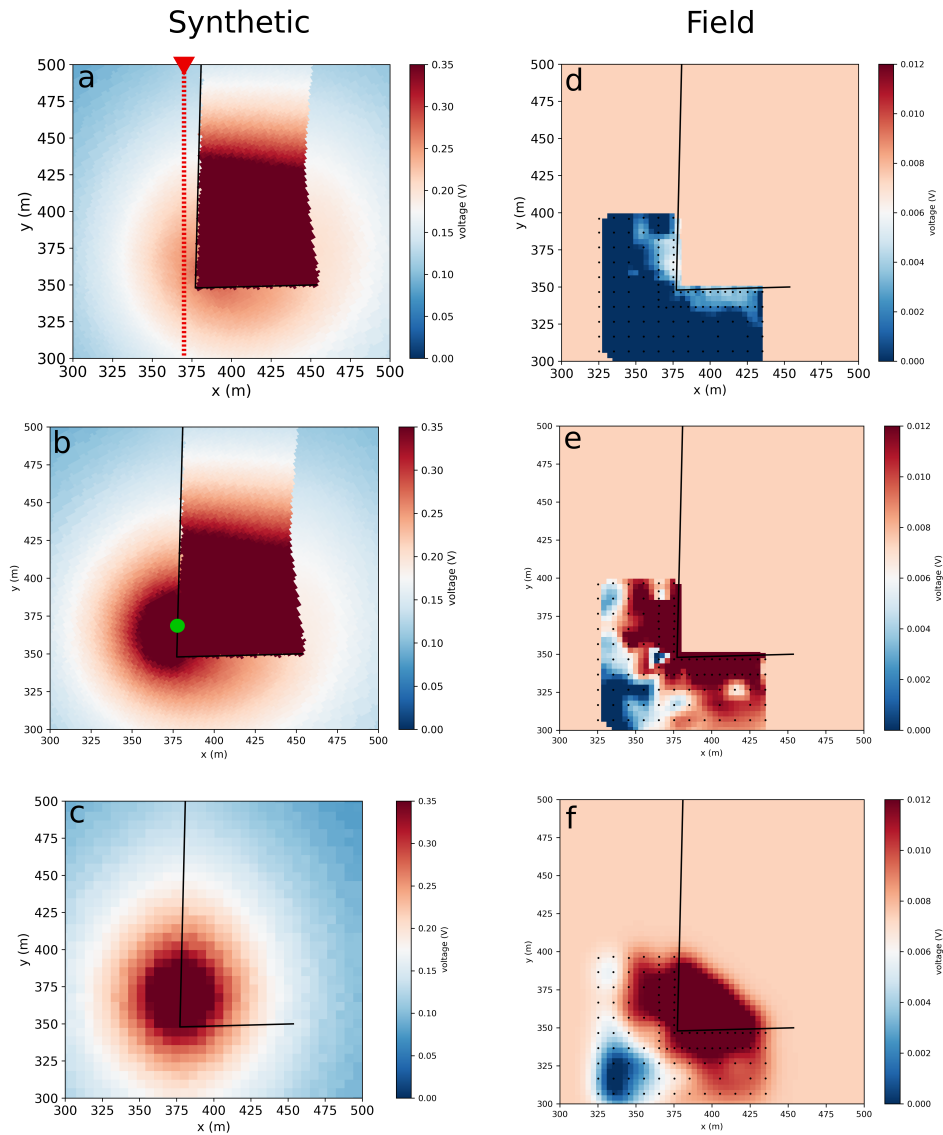


Figure 2. normalised voltage distribution (voltage/injected current) at the ground surface for synthetic data (left column) and field data (right column). (a) and (b) show respectively the simulated normalized voltage for an intact liner and for a perforated liner (the green point indicates the position of a hole 10 m wide and 8 m high, with its top at -12.5 m from the ground), and (c) after mirroring (section Supporting Information). (d) and (e) show the raw data for the field case respectively before (d), after (e) correction for the influence of the return electrode, and (f) after correction for B + Gaussian smoothing (see Supporting Information). The red dashed line indicate the profile used for the DEXP analysis in fig 3.

239
240
241
242

this study the position of the current electrode was placed very close to the leakage point. The conductive nature of the inner landfill material reduces the effect of the actual location of the current location point, and conveys current towards the leak. The source producing the electrical potential is thus linked to the current circulation in

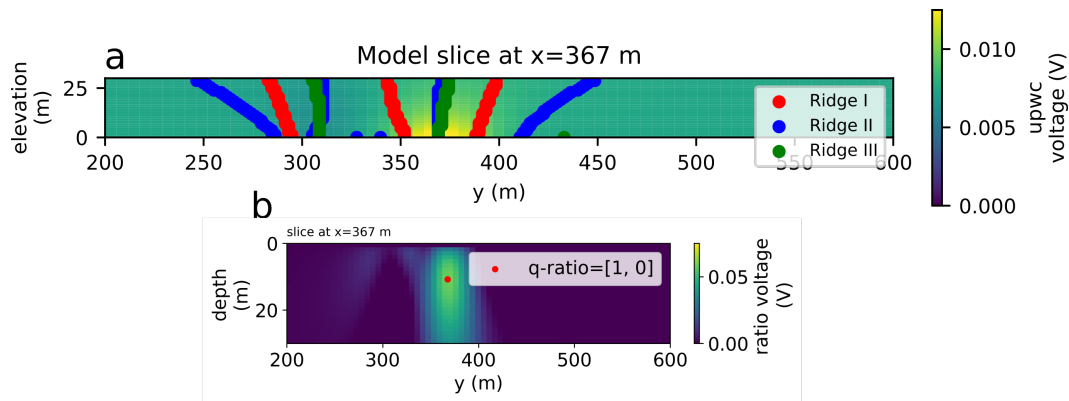


Figure 3. (a) upward continued section of the field data and its ridges lines from searches for zeros of ridges RI, RII and RIII (see SI). (b) DEXP transformation using the automatic ratio method between the derivative of order 1 and 0; the maximum (red dot) indicates the source depth estimate.

243 the conductive body. As the MALM assumption relies on the fact that the conductive
 244 body is much more conductive with respect to the surrounding medium, we tested this
 245 assumption against the potential field imaging theory. Note that our MALM approach
 246 is aimed at identifying the source not the conductive body extent.

247 The location of the MALM (A) electrode far from the leakage point would lead
 248 to a wrong estimate of the leak position. When moving A, most of the current spreads
 249 out under the liner instead of going through the hole (figure not shown). The potential
 250 field distribution is alike to a no-hole configuration and applying the DEXP procedure
 251 results in a wrong estimate of the depth. Considering the complex geometry of the
 252 landfill, a 3d DEXP analysis would help to identify the source position and depth.
 253 Indeed, running a 3d analysis would allow better discrimination between the residual
 254 background signal due to the current going under the landfill and the current going
 255 into the hole.

256 Here for simplicity and by lack of data, although most likely the subsurface was
 257 heterogeneous due to highly conductive leachates relative to surrounding groundwater,
 258 we assumed an homogeneous soil during the correction of the influence of the electrode
 259 N position. In a preliminary study we found that the effect of the initial resistivity
 260 model i.e. the contrast of conductivity between the body and its surrounding medium
 261 does not affect the source depth position identification up to three orders of magnitude
 262 differences (see Supporting Information). This is in-line with Mauri et al. (2010) who
 263 show a similar result for the CWT case applied to SP signals (that is also conditioned
 264 by the electrical resistivity distribution). Also varying the noise level and source depth
 265 showed respectively no effect and small errors on the source depth detection using the
 266 DEXP ratio analysis.

267 An important limiting factor of the potential field theory is the choice of the
 268 Structural Index matching the anomaly shape (Stavrev & Reid, 2007) which ultimately
 269 guides the choice of the depth weighting factor. This can be very difficult to assess in
 270 complex field sites. In the case of a landfill leakage, however, this is a minor problem as
 271 the anomaly can be considered point-like and isolated. This could explain why for the
 272 synthetic cases the estimated source parameters show very good agreement with the
 273 “true” values (both for gravimetric and MALM data – see Supporting Information).

274 An important issue to consider relates to the presence of domain boundaries. In
275 a simple case, the only electrical boundary to consider is the soil/air interface. In the
276 specific case of the described landfill, it is necessary to deal with the liner boundary. We
277 removed the influence of the liner boundary by mirroring the data around the boundary
278 before applying the upward continuation of the field. The outside part of the landfill
279 was mirrored against a line parallel to the landfill side. The step is validated via
280 synthetic modelling (see SI material) where the source depth was correctly estimated.
281 Correcting for the pole source is most of the time not required for field application of
282 MALM; and in other cases a reasonable estimation of electrical resistivity distribution
283 can be obtained from ERT – in this case the correction is not really needed due to
284 the homogenizing effect of the brackish water high electrical conductivity. Note that
285 the survey described in this paper was likely the most penalizing case that we could
286 encounter for leakage detection: for some cases the landfill is accessible and the remote
287 electrode can be placed far away to avoid the correction step. For these other easier
288 cases less refined strategies shall be applied.

289 This study shows that the estimation of source locations can be biased by a few
290 factors, and in particular: (i) the quality of the data (ii) the stability of the upward
291 continuation and of its spatial derivatives. About these factors, first of all, we note
292 that the noise is confined to low elevations, due to the well-known smoothing effect
293 of the upward continuation operator in the DEXP transformation. This noise was
294 successfully removed fitting the ridges to a given range of altitudes. While an efficient
295 way to isolate the anomalies is to vary the order of the differentiation of the field (which
296 can be safely done thanks to the smoothing properties of the upward continuation), in
297 this study the anomaly was easily identified only using the ratio between the first and
298 the upward continued field.

299 This approach overcomes some limitations of the classical inversion, yet potential
300 field methods are subject to bias just like any other geophysical inverse problem. The
301 potential field imaging of MALM does not converge perfectly to the exact location of
302 sources if the resistivity model is very complex. At most, an approximate (and yet
303 very useful) source location is identified. This is expected consistently with literature
304 evidence. The best approach that can limit the natural uncertainty in source identi-
305 fication is the use of synthetic modelling, based on solid assumptions concerning the
306 expected anomalies distributions and source locations. The results of these exercises
307 become fundamental in supporting the interpretation of the MALM results.

308 6 Conclusions

309 This study presents a successful application of MALM, a well-established geo-
310 electrical method, using a novel processing approach. The information content of
311 MALM is fully exploited using the potential field imaging theory. The results we
312 present are relevant to both a synthetic study and a field case. The synthetics indicate
313 that the proposed approach can estimate the source depth accurately considering a
314 correction of the influence of the remote current return electrode. The field application
315 exploited the theory to estimate the leak depth from a damaged landfill. Synthetic
316 modelling reproducing the actual field conditions shows that an hole into the liner
317 where the current can leak can be seen both from the multi-ridge analysis and DEXP.
318 For the real case, the source depth analysis shows similar results than the damaged
319 synthetic modeling.

320 Data availability statement

321 Codes and data to reproduce figures articles are available in the Zenodo data
322 repository (10.5281/zenodo.6538070) and in to the Github (https://github.com/BenjMy/dEXP_imaging/tree/master)

Acknowledgments

The authors thank L. Slater and the anonymous reviewers for their constructive comments on the manuscript. This project has received funding from the European Union's Horizon 2020 research and innovation programme under the Marie Skłodowska-Curie grant agreement No 842922. We acknowledge financial support from the Italy-Israel bilateral project ECZ-Dry.

References

- Abbas, M. A., & Fedi, M. (2014, December). Automatic DEXP imaging of potential fields independent of the structural index. *Geophysical Journal International*, *199*(3), 1625–1632. Retrieved 2020-10-06, from <https://academic.oup.com/gji/article/199/3/1625/617350> (Publisher: Oxford Academic) doi: 10.1093/gji/ggu354
- Abbas, M. A., Fedi, M., & Florio, G. (2014, December). Improving the local wavenumber method by automatic DEXP transformation. *Journal of Applied Geophysics*, *111*, 250–255. Retrieved 2020-05-04, from <https://linkinghub.elsevier.com/retrieve/pii/S0926985114002900> doi: 10.1016/j.jappgeo.2014.10.004
- Abdelrahman, E. M., El-Araby, T. M., Abo-Ezz, E. R., Soliman, K. S., & Essa, K. S. (2008, May). A New Algorithm for Depth Determination from Total Magnetic Anomalies due to Spheres. *Pure and Applied Geophysics*, *165*(5), 967–979. Retrieved 2021-09-21, from <https://doi.org/10.1007/s00024-008-0340-x> doi: 10.1007/s00024-008-0340-x
- Agarwal, B. N. P., & Srivastava, S. (2009, November). Analyses of self-potential anomalies by conventional and extended Euler deconvolution techniques. *Computers & Geosciences*, *35*(11), 2231–2238. Retrieved 2021-09-21, from <https://doi.org/10.1016/j.cageo.2009.03.005> doi: 10.1016/j.cageo.2009.03.005
- Baniamerian, J., Fedi, M., & Oskooi, B. (2016, September). Research Note: Compact Depth from Extreme Points: a tool for fast potential field imaging: Compact depth from extreme points. *Geophysical Prospecting*, *64*(5), 1386–1398. Retrieved 2020-10-06, from <http://doi.wiley.com/10.1111/1365-2478.12365> doi: 10.1111/1365-2478.12365
- Bhattacharya, B. B., & Roy, N. (1981). A Note on the Use of a Nomogram for Self-Potential Anomalies*. *Geophysical Prospecting*, *29*(1), 102–107. Retrieved 2021-09-21, from <https://onlinelibrary.wiley.com/doi/abs/10.1111/j.1365-2478.1981.tb01013.x> (eprint: <https://onlinelibrary.wiley.com/doi/pdf/10.1111/j.1365-2478.1981.tb01013.x>) doi: 10.1111/j.1365-2478.1981.tb01013.x
- Binley, A., Daily, W., & Ramirez, A. (1999). Detecting Leaks from Waste Storage Ponds using Electrical Tomographic Methods. , 8.
- Binley, A., Ramirez, A., & Daily, W. (1995). Regularised image reconstruction of noisy electrical resistance tomography data. In *Proceedings of the 4th Workshop of the European Concerted Action on Process Tomography, Bergen, Norway* (pp. 401–410).
- Blakely, R. J. (1995). *Potential Theory in Gravity and Magnetic Applications*. Cambridge: Cambridge University Press. Retrieved 2020-10-06, from <https://www.cambridge.org/core/books/potential-theory-in-gravity-and-magnetic-applications/348880F23008E16E663D6AD14A41D8DE> doi: 10.1017/CBO9780511549816
- De Carlo, L., Perri, M. T., Caputo, M. C., Deiana, R., Vurro, M., & Cassiani, G. (2013, November). Characterization of a dismissed landfill via electrical resistivity tomography and mise-la-masse method. *Journal of Applied Geophysics*, *98*, 1–10. Retrieved 2020-03-16, from <https://linkinghub.elsevier.com/>

- 376 retrieve/pii/S0926985113001493 doi: 10.1016/j.jappgeo.2013.07.010
 377 de Villiers, G., Ridley, K., Rodgers, A., & Boddice, D. (2019, November). On
 378 the use of the profiled singular-function expansion in gravity gradiometry.
 379 *Journal of Applied Geophysics*, *170*, 103830. Retrieved 2020-05-04, from
 380 <https://linkinghub.elsevier.com/retrieve/pii/S0926985118310437>
 381 doi: 10.1016/j.jappgeo.2019.103830
- 382 Fedi, M. (2007, January). DEXP: A fast method to determine the depth and the
 383 structural index of potential fields sources. *Geophysics*, *72*(1), I1–I11. Re-
 384 trieved 2020-05-04, from <http://library.seg.org/doi/10.1190/1.2399452>
 385 doi: 10.1190/1.2399452
- 386 Fedi, M., Cella, F., Quarta, T., & Villani, A. V. (2010, May). 2D Continuous
 387 Wavelet Transform of potential fields due to extended source distributions.
 388 *Applied and Computational Harmonic Analysis*, *28*(3), 320–337. Retrieved
 389 2021-03-02, from [https://www.sciencedirect.com/science/article/pii/](https://www.sciencedirect.com/science/article/pii/S1063520310000308)
 390 [S1063520310000308](https://www.sciencedirect.com/science/article/pii/S1063520310000308) doi: 10.1016/j.acha.2010.03.002
- 391 Fedi, M., Florio, G., & Cascone, L. (2007, June). Improved SCALFUN Analy-
 392 sis of Potential Fields by a Criterion of RidgeConsistency. In (pp. cp–27–
 393 00183). European Association of Geoscientists & Engineers. Retrieved
 394 2020-10-06, from [https://www.earthdoc.org/content/papers/10.3997/](https://www.earthdoc.org/content/papers/10.3997/2214-4609.201401601)
 395 [2214-4609.201401601](https://www.earthdoc.org/content/papers/10.3997/2214-4609.201401601) (ISSN: 2214-4609) doi: 10.3997/2214-4609.201401601
- 396 Fedi, M., & Pilkington, M. (2012, January). Understanding imaging methods
 397 for potential field data. *Geophysics*, *77*(1), G13–G24. Retrieved 2020-05-
 398 04, from <http://library.seg.org/doi/10.1190/geo2011-0078.1> doi:
 399 10.1190/geo2011-0078.1
- 400 Florio, G., & Fedi, M. (2018, May). Depth estimation from downward continu-
 401 ation: An entropy-based approach to normalized full gradient. *Geophysics*,
 402 *83*(3), J33–J42. Retrieved 2020-05-04, from [https://library.seg.org/doi/](https://library.seg.org/doi/10.1190/geo2016-0681.1)
 403 [10.1190/geo2016-0681.1](https://library.seg.org/doi/10.1190/geo2016-0681.1) doi: 10.1190/geo2016-0681.1
- 404 Gibert, D., & Pessel, M. (2001, May). Identification of sources of potential fields
 405 with the continuous wavelet transform: Application to self-potential profiles.
 406 *Geophysical Research Letters*, *28*(9), 1863–1866. Retrieved 2021-09-21, from
 407 <https://hal-insu.archives-ouvertes.fr/insu-03324637> (Publisher:
 408 American Geophysical Union) doi: 10.1029/2000GL012041
- 409 Lapenna, V., Patella, D., Piscitelli, S., et al. (2000). Tomographic analysis of self-
 410 potential data in a seismic area of southern Italy. *Annali di Geofisica*, *d3*, 361-
 411 373.
- 412 Ling, C., Revil, A., Qi, Y., Abdulsamad, F., Shi, P., Nicaise, S., & Peyras, L. (2019,
 413 November). Application of the Mise-la-Masse method to detect the bot-
 414 tom leakage of water reservoirs. *Engineering Geology*, *261*, 105272. Re-
 415 trieved 2020-04-28, from [https://linkinghub.elsevier.com/retrieve/pii/](https://linkinghub.elsevier.com/retrieve/pii/S0013795219311305)
 416 [S0013795219311305](https://linkinghub.elsevier.com/retrieve/pii/S0013795219311305) doi: 10.1016/j.enggeo.2019.105272
- 417 Liu, S., Baniamerian, J., & Fedi, M. (2020, May). Imaging Methods Ver-
 418 sus Inverse Methods: An Option or An Alternative? *IEEE Transactions*
 419 *on Geoscience and Remote Sensing*, *58*(5), 3484–3494. Retrieved 2020-
 420 04-29, from <https://ieeexplore.ieee.org/document/8941065/> doi:
 421 10.1109/TGRS.2019.2957412
- 422 Mary, B., Peruzzo, L., Boaga, J., Cenni, N., Schmutz, M., Wu, Y., ... Cassiani,
 423 G. (2020, March). Time-lapse monitoring of root water uptake using elec-
 424 trical resistivity tomography and mise-la-masse: a vineyard
 425 infiltration experiment. *SOIL*, *6*(1), 95–114. Retrieved 2020-03-16, from
 426 <https://www.soil-journal.net/6/95/2020/> doi: 10.5194/soil-6-95-2020
- 427 Mary, B., Peruzzo, L., Boaga, J., Schmutz, M., Wu, Y., Hubbard, S. S., & Cassiani,
 428 G. (2018, October). Small-scale characterization of vine plant root water
 429 uptake via 3-D electrical resistivity tomography and mise-la-masse method.
 430 *Hydrology and Earth System Sciences*, *22*(10), 5427–5444. Retrieved 2019-10-

- 431 17, from <https://www.hydrol-earth-syst-sci.net/22/5427/2018/> doi:
432 10.5194/hess-22-5427-2018
- 433 Mauri, G., Williams-Jones, G., & Saracco, G. (2010, April). Depth determina-
434 tions of shallow hydrothermal systems by self-potential and multi-scale wavelet
435 tomography. *Journal of Volcanology and Geothermal Research*, 191(3), 233–
436 244. Retrieved 2020-10-14, from [http://www.sciencedirect.com/science/
437 article/pii/S0377027310000387](http://www.sciencedirect.com/science/article/pii/S0377027310000387) doi: 10.1016/j.jvolgeores.2010.02.004
- 438 Parasnis, D. S. (1967, April). Three-dimensional electric mise-a-la-masse survey of
439 an irregular lead-zinc-copper deposit in central sweden. *Geophysical Prospect-*
440 *ing*, 15(3), 407–437. Retrieved 2020-10-06, from [https://www.earthdoc.org/
441 content/journals/10.1111/j.1365-2478.1967.tb01796.x](https://www.earthdoc.org/content/journals/10.1111/j.1365-2478.1967.tb01796.x) (Pub-
442 lisher: European Association of Geoscientists & Engineers) doi: 10.1111/
443 j.1365-2478.1967.tb01796.x
- 444 Patella, D. (1997). Introduction to ground surface self-potential tomography. *Geo-*
445 *physical Prospecting*, 45(4), 653–681.
- 446 Perri, M. T., De Vita, P., Masciale, R., Portoghese, I., Chirico, G. B., & Cassiani,
447 G. (2018, June). Time-lapse Mise--la-Masse measurements and modeling
448 for tracer test monitoring in a shallow aquifer. *Journal of Hydrology*, 561,
449 461–477. Retrieved 2020-03-16, from [https://linkinghub.elsevier.com/
450 retrieve/pii/S0022169417307679](https://linkinghub.elsevier.com/retrieve/pii/S0022169417307679) doi: 10.1016/j.jhydrol.2017.11.013
- 451 Peruzzo, L., Chou, C., Wu, Y., Schmutz, M., Mary, B., Wagner, F. M., ... Hub-
452 bard, S. (2020, May). Imaging of plant current pathways for non-invasive
453 root Phenotyping using a newly developed electrical current source den-
454 sity approach. *Plant and Soil*, 450(1-2), 567–584. Retrieved 2020-07-14,
455 from <http://link.springer.com/10.1007/s11104-020-04529-w> doi:
456 10.1007/s11104-020-04529-w
- 457 Revil, A. (2013, July). Comment on A fast interpretation of self-potential data using
458 the depth from extreme points method (M. Fedi and M. A. Abbas, 2013, Geo-
459 physics, 78, no.2, E107E116). *Geophysics*, 78(4), X1–X7. Retrieved 2020-10-06,
460 from <https://library.seg.org/doi/abs/10.1190/geo2013-0052.1> (Pub-
461 lisher: Society of Exploration Geophysicists) doi: 10.1190/geo2013-0052.1
- 462 Saracco, G., Labazuy, P., & Moreau, F. (2004). Localization of self-potential
463 sources in volcano-electric effect with complex continuous wavelet trans-
464 form and electrical tomography methods for an active volcano. *Geophysical*
465 *Research Letters*, 31(12). Retrieved 2020-10-06, from [https://agupubs
466 .onlinelibrary.wiley.com/doi/abs/10.1029/2004GL019554](https://agupubs.onlinelibrary.wiley.com/doi/abs/10.1029/2004GL019554) (eprint:
467 <https://agupubs.onlinelibrary.wiley.com/doi/pdf/10.1029/2004GL019554>) doi:
468 10.1029/2004GL019554
- 469 Schlumberger, C. (1920). *tude sur la prospection lectrique du sous-sol*. Gauthier-
470 Villars. (Google-Books-ID: fhYxAAAAMAAJ)
- 471 Shao, Z., Revil, A., Mao, D., & Wang, D. (2018, April). Finding buried metallic
472 pipes using a non-destructive approach based on 3D time-domain induced
473 polarization data. *Journal of Applied Geophysics*, 151, 234–245. Retrieved
474 2020-03-16, from [https://linkinghub.elsevier.com/retrieve/pii/
475 S0926985118301678](https://linkinghub.elsevier.com/retrieve/pii/S0926985118301678) doi: 10.1016/j.jappgeo.2018.02.024
- 476 Soueid Ahmed, A., Jardani, A., Revil, A., & Dupont, J. (2013, September).
477 SP2DINV: A 2D forward and inverse code for streaming potential prob-
478 lems. *Computers & Geosciences*, 59, 9–16. Retrieved 2020-04-23, from
479 <https://linkinghub.elsevier.com/retrieve/pii/S00983300413001507>
480 doi: 10.1016/j.cageo.2013.05.008
- 481 Srivastava, S., & Agarwal, B. N. P. (2010, June). Inversion of the amplitude
482 of the two-dimensional analytic signal of the magnetic anomaly by the
483 particle swarm optimization technique: Inversion of AAS by PSO. *Geo-*
484 *physical Journal International*, 182(2), 652–662. Retrieved 2021-09-21,
485 from <https://academic.oup.com/gji/article-lookup/doi/10.1111/>

- 486 j.1365-246X.2010.04631.x doi: 10.1111/j.1365-246X.2010.04631.x
487 Stavrev, P., & Reid, A. (2007, January). Degrees of homogeneity of potential
488 fields and structural indices of Euler deconvolution. *Geophysics*, 72(1),
489 L1–L12. Retrieved 2021-09-21, from [https://library.seg.org/doi/abs/
490 10.1190/1.2400010](https://library.seg.org/doi/abs/10.1190/1.2400010) (Publisher: Society of Exploration Geophysicists) doi:
491 10.1190/1.2400010
492 Wondimu, H. D., Mammo, T., & Webster, B. (2018, October). 3D joint inversion
493 of Gradient and Mise--la-Masse borehole IP/Resistivity data and its applica-
494 tion to magmatic sulfide mineral deposit exploration. *Acta Geophysica*, 66(5),
495 1031–1045. Retrieved 2020-03-16, from [http://link.springer.com/10.1007/
496 s11600-018-0199-x](http://link.springer.com/10.1007/s11600-018-0199-x) doi: 10.1007/s11600-018-0199-x